Nanoporous alumina enhanced surface plasmon resonance sensors

Alexandros G. Koutsioubas, Nikolaos Spiliopoulos, Dimitris Anastassopoulos, Alexandros A. Vradis,[a] and George D. Priftis
Department of Physics, University of Patras, GR 26 500, Greece

(Received 13 September 2007; accepted 15 March 2008; published online 13 May 2008)

The signal enhancement of an easy to fabricate, nanoporous alumina assisted surface plasmon resonance (SPR) sensor is investigated. It is theoretically shown that the presence of a thin (under 200 nm) porous alumina layer on top of an aluminum film supporting the surface plasmons, may significantly increase (over one order of magnitude) the sensitivity of the SPR method in the case where the adsorption of relatively small molecules is probed. The comparative experimental investigation of self-assembled monolayer formation on planar metal films and porous alumina layers verifies the theoretical predictions. Based on these results, we discuss the extended applicability of this setup in biosensor and other related applications. © *2008 American Institute of Physics*. [DOI: 10.1063/1.2924436]

I. INTRODUCTION

Plasmonics is currently a fast growing field with enormous potential applications in the areas of optical computing, novel optical devices, and medical/biological research.[1] Surface plasmon resonance spectroscopy (SPRS) is a well established optical technique involving the excitation of coherent oscillations of the free electrons on a metal/dielectric boundary. Under the widely implemented Kretchmann configuration,[2,3] surface plasmons (SPs) are excited by an evanescent electromagnetic wave, generated by incidence of light on the face of a metal coated prism, under total internal reflection conditions. The properties of SPs are highly dependent on the refractive index of the adjacent medium within distances of about 200 nm from the metal surface. This fact has enabled the use of SPRS in a wide range of surface studies and especially as a biosensor for the detection of binding effects.[4,5]

Anodically etched porous alumina (p-Al_2O_3) is a new, interesting material for the development of ordered structures at the nanometer scale.[6] During the anodization under specific conditions,[7] highly regular pore structures are formed, self-organizing in hexagonal arrays. Porous alumina has been recently used as a template for the formation of nanowires,[8,9] nanodots,[10] and in various sensor applications.[11,12] The anodization of aluminum thin films as opposed to foils has been also investigated.[13] In general, sensors based on porous media take advantage of the fact that pore formation is associated with a large increase of the sensing surface that boosts the measurable signal.

In 2004, Lau *et al.*[14] proposed a metal-cladded p-Al_2O_3 waveguide based sensor operating under the same Kretschmann geometry. This sensor provides a very high sensitivity to molecules adsorbed within the porous layer and has been followed by other works involving the use of thick porous layers of various types, such as, nanoporous TiO_2 films[15,16] and block copolymer films with cylindrical microdomains.[17]

In the present work, we investigate in detail the integration of a thin porous layer in classic SP resonance (SPR) sensors, operating in nonwaveguide mode. The proposed setup configuration involves a thin (under 200 nm) nanoporous alumina layer, grown on top of an aluminum thin film supporting surface plasmon excitations. The already sensitive surface plasmon response is greatly enhanced by the increased available surface for the adsorption of incoming molecules.

II. THEORY

The structure of the sensing configuration is illustrated in Fig. 1. We assume a typical Kretschmann configuration for the excitation of SPs on a thin aluminum film under the presence of a porous alumina adlayer.

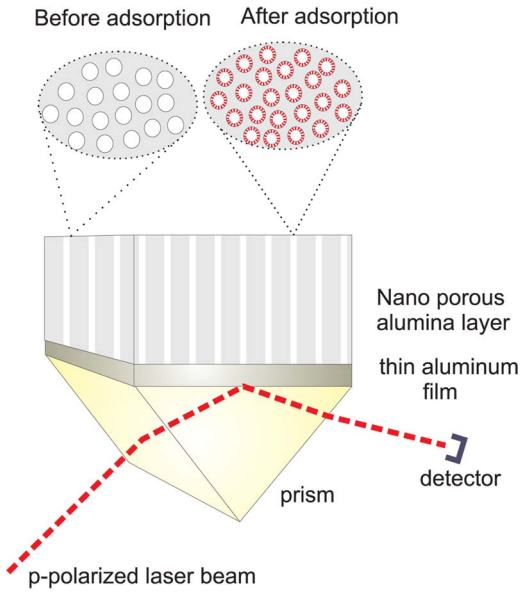

FIG. 1. (Color online) Schematic illustration of the nanoporous alumina assisted SPR setup. Two "magnified" illustrations of the p-Al_2O_3 surface before and after the formation of a thin layer on the pore walls are shown at the top.

[a]Electronic mail: vradis@physics.upatras.gr.

Theoretical calculations of SPR curves (reflected light intensity versus angle of incidence) for the four layer system (prism/aluminum/porous alumina/air) are carried out by application of the matrix formalism for homogeneous stratified dielectric media. The system is modeled as a stack of optically homogeneous layers, characterized by their thickness and complex dielectric constant.

Since the incident light and plasmon wavelengths[18] are much larger than the characteristic features of porous alumina used in our experiments (e.g., pore diameter, interpore distance), the theoretical treatment of the dielectric function of the porous medium is based on the cavity Maxwell–Garnett (c-MG) effective medium approximation.[19] In the case where the pores are filled with air, the dielectric constant of the porous alumina layer $\varepsilon_{p\text{-}Al_2O_3}$ is given by

$$\varepsilon_{p\text{-}Al_2O_3} = \frac{2(1-f)\varepsilon_{Al_2O_3}^2 + (1+2f)\varepsilon_{Al_2O_3}}{1-f+(2+f)\varepsilon_{Al_2O_3}}, \quad (1)$$

where f is the pore volume fraction and $\varepsilon_{Al_2O_3}$ the dielectric constant of bulk alumina.

In order to incorporate the contribution of adsorbed molecules on the pore walls to the effective dielectric constant, a modification of the c-MG theory is required[19] for the modeling of a dielectric mixture consisting of three constituent materials, two of which are related. The topology of this mixture (Fig. 1, top) is comprised of a core (air pores) with a dielectric function ($\varepsilon_{air}=1$), a surrounding shell (adsorbed molecules), and the alumina surrounding medium. The effective dielectric constant ε_{eff} of this three-component mixture is given by[19]

$$\varepsilon_{eff} = \frac{fA_c\rho^3 + f\varepsilon_s A_s(1-\rho^3) + \varepsilon_{Al_2O_3}(1-f)}{fA_c\rho^3 + fA_s(1-\rho^3) + 1 - f}, \quad (2)$$

where $A_c=3\varepsilon_s B$, $A_s=(3+2\varepsilon_s)B$, $\rho=r_c/r_s$, and

$$B = \frac{3\varepsilon_{Al_2O_3}}{(\varepsilon_s+2\varepsilon_{Al_2O_3})(2\varepsilon_s+1) - 2(\varepsilon_s-\varepsilon_{Al_2O_3})(\varepsilon_s-1)\rho^3},$$

where ε_s the dielectric constant of the shell, (adsorbed molecules on the pore wall), r_c and r_s are the radii of the core and shell respectively, and f is the total volume fraction of the cores and shells.

Typical SPRS applications involve the detection of changes of the angular position of the reflected intensity minimum (θ_{min}) under the influence of an adsorbed layer on the metal film surface. The magnitude of the shift of θ_{min} ($\Delta\theta_{min}$), in respect to its position before the adsorption of the layer, determines the sensitivity of the sensor.

When aluminum thin films are used for the SP excitation, adsorption phenomena may be studied on the ultrathin natural alumina layer that is formed on the aluminum film. For the system [SF10 prism/aluminum 15 nm/Al_2O_3 (3 nm)/air], the shift of θ_{min} after the formation of an adsorbed layer with refractive index $n_s=1.5$ and thickness $d_s=2$ nm is $\Delta\theta_{min}=0.11°$. In the case of a planar gold SPR sensor [SF10 prism/gold (50 nm)/air], the shift of θ_{min} after the formation of the same adsorbed layer is $\Delta\theta_{min}=0.21°$.

TABLE I. Theoretically calculated changes in the reflectivity minimum $\Delta\theta_{min}$ due to the formation of a 2 nm layer of refractive index $n=1.5$ on the pore walls for two sets of p-Al_2O_3 layer parameters. The parameters of the second column are close to those used in our experiments, while parameters of the third column correspond to a p-Al_2O_3 layer of higher porosity and larger pore size (Ref. 27).

p-Al_2O_3 layer thickness (nm)	$\Delta\theta_{min}$ (pore radius=7.5 nm, pore density=5×10^{10} cm^{-2})	$\Delta\theta_{min}$ (pore radius=12 nm, pore density=8×10^{10} cm^{-2})
50	0.41°	0.91°
100	1.60°	3.13°
150	2.23°	4.45°
200	2.52°	4.99°

Now assuming that the same layer is formed on the pore walls of a nanoporous alumina adlayer, forming a shell that separates air pores and alumina and based on the above theoretical treatment, we can calculate the shift in θ_{min} that is induced by adsorption. In Table I, we present results of these calculations for a pore density equal to 5×10^{10} pores/cm^2 (Fig. 2) and 8×10^{10} pores/cm^2 (Fig. 3), for two different pore radii of 7.5 and 12 nm, and various pore depths d ranging from 50 to 200 nm which cover the full probing range of SPs.

We observe that the calculated $\Delta\theta_{min}$ values in Table I are quite high while they are an ascending function of pore radius and depth. For optimum parameters of the porous medium, $\Delta\theta_{min}$ is over 45 times higher compared to the shift of θ_{min} for adsorption on a planar alumina surface and 22 times higher compared to the shift of θ_{min} for adsorption on a gold film (Fig. 4). Analogous sensitivity enhancement but reduced by roughly a factor of 2 is predicted for *in situ* measurements where the porous alumina layer is in contact with a liquid medium of refractive index equal to 1.33.

Another useful figure of merit for the estimation of the sensitivity is the ratio of the shift in the position of the resonance dip divided by the width of that dip. That is because the presence of the p-Al_2O_3 layer widens the reflectivity curve, making the drop in reflectivity less pronounced. Even using this stricter figure of merit, we still find that the optimum p-Al_2O_3 layer gives more than an order of magnitude better sensitivity compared to the planar sensor geometry.

III. EXPERIMENTAL

In order to check these theoretical arguments, we have chosen a relatively simple procedure for the fabrication of nanoporous alumina adlayers over thin aluminum films that support the excitation of SPs.

Briefly, optically flat SF10 slides ($n_{SF10}=1.723$) were used as supports, which were cleaned by overnight exposure to fresh sulfochromic acid and then rinsed with de-ionized water and ethanol. Aluminum layers of thickness between 70 and 95 nm were deposited on the SF10 slides by vacuum evaporation of 99.999% pure aluminum wire at a base pressure of 1×10^{-6} Torr and at a deposition rate of 0.6 nm/s. Then partial anodization of aluminum films was carried out following the procedure proposed by Miney *et al.*[20] The samples were anodized in a 0.3*M* sulfuric acid aqueous solution, under a constant voltage 20 V at 283±0.5 K while

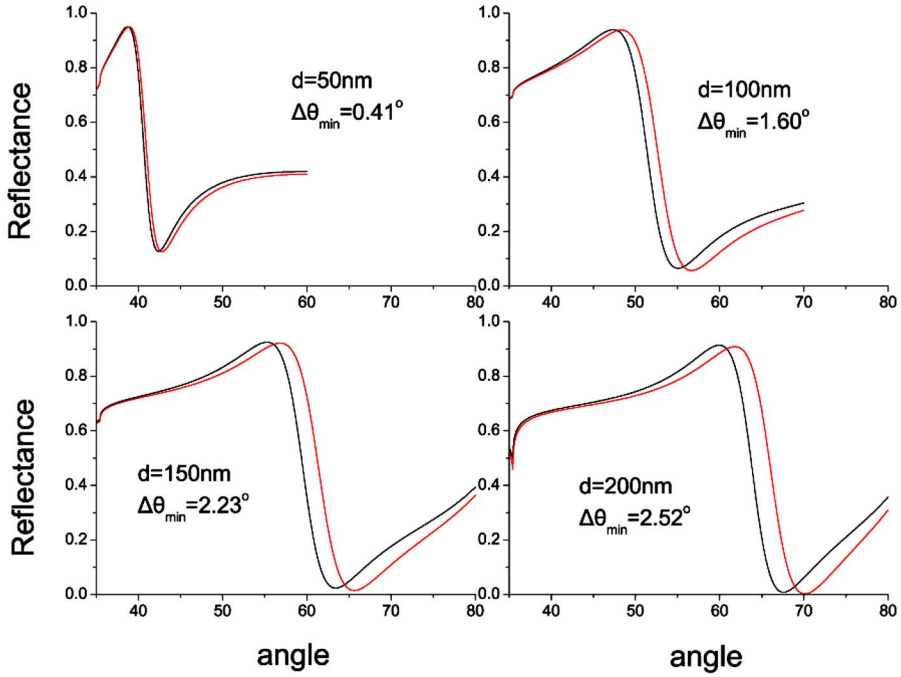

FIG. 2. (Color online) Theoretical SPR curves, illustrating the large shift that is induced by the formation of a thin (2 nm) organic film on the pore walls of p-Al_2O_3 layers of various thicknesses d. The thickness of the aluminium SP supporting film is 15 nm. While the p-Al_2O_3 pore density is set equal to 5×10^{10} cm^{-2} and pore radius equal to 7.5 nm.

the electrolyte was magnetically stirred. After anodization, each sample was rinsed with de-ionized water, pure ethanol, and dried under a stream of dry nitrogen.

In Fig. 5, we present the typical behavior of the measured current during the anodization process for the growth of a nanoporous alumina layer. Four different phases in the anodization procedure can be distinguished. After an initial sharp decrease in current (phase A) due to the formation of a thin oxide film, the current increases due to pore nucleation (phase B). Then the current remains relatively stable (phase C) as the rate of pore growth becomes constant. Finally, the current drops rapidly (phase D) when the last few nanometers of aluminum are consumed. For Al films thinner than 50 nm, we have found that the anodization current starts to fall before a stable pore growth rate is achieved, so phase C is not clearly observed.

Each anodization process was terminated ~5 s after the onset of phase D, in order to leave a relatively uniform[21] aluminum film of about 9 ± 2 nm under the p-Al_2O_3 layer, each anodization process was terminated ~5 s after the onset of phase D. We have found that the behavior of the current is reproducible for films that have the same thickness.

The morphology of the anodized films was characterized using a Jeol JSM-5200 scanning electron microscope (SEM). Figure 6 shows a micrograph of the surface of an aluminum film after partial anodization. Since our films are too thin and only a single anodization step is performed, high pore uniformity and strict hexagonal ordering are not observed.[9,13] The mean pore radius is about 7–8 nm and pore density is estimated to be about 5×10^{10} pores/cm^2. After anodization, the oxidized p-Al_2O_3 layer is about 1.5 times thicker than the initial Al film. This fact has been observed by acquiring cross

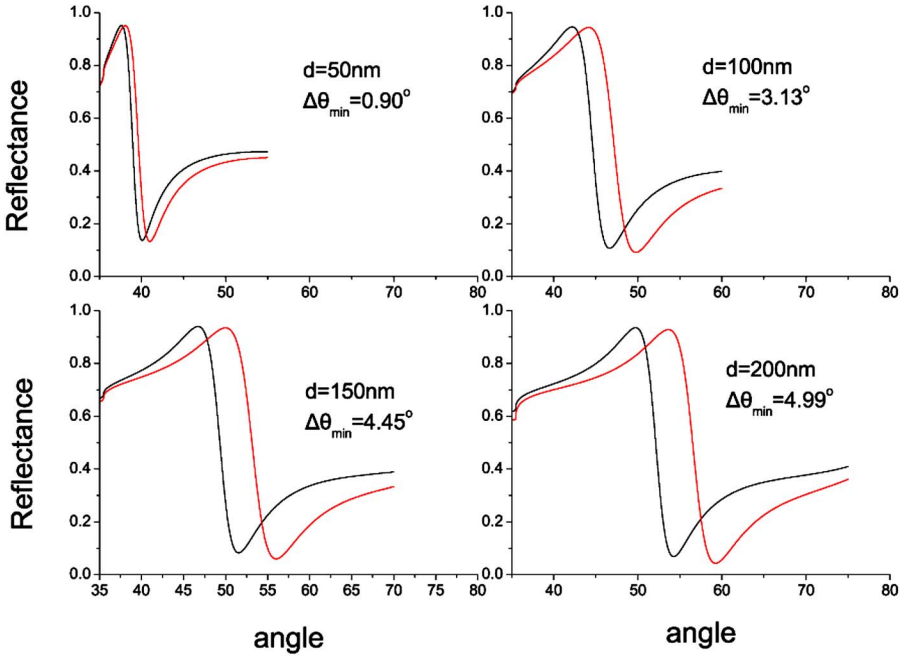

FIG. 3. (Color online) Theoretical calculations as those presented in Fig. 2, for a p-Al_2O_3 layer of 8×10^{10} cm^{-2} pore density and 12 nm pore thickness.

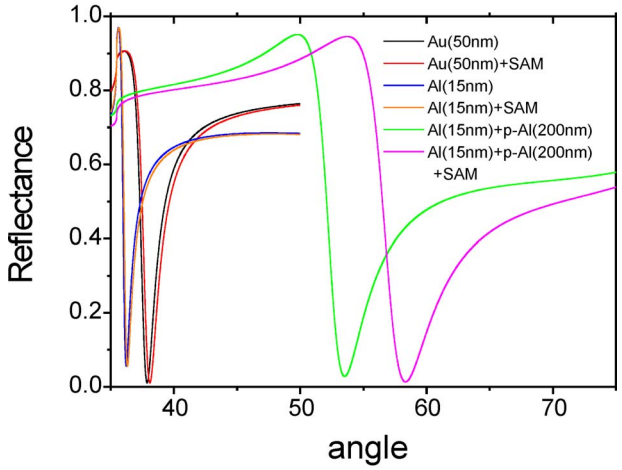

FIG. 4. (Color online) Theoretically calculated curves, comparing (planar aluminum, planar gold, and porous alumina assisted) SPR sensor response that is induced by the adsorption of a 2 nm organic layer.

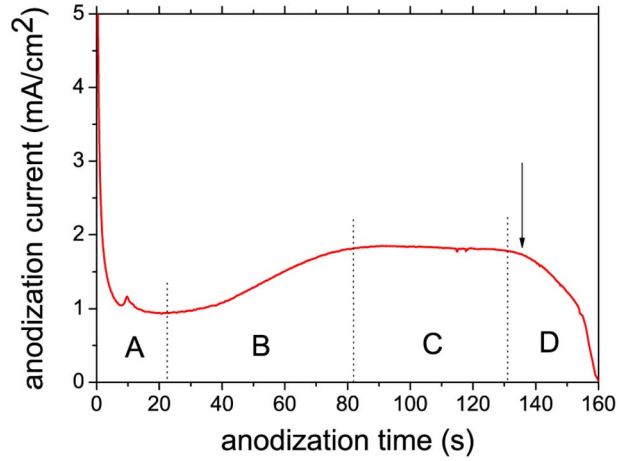

FIG. 5. (Color online) Typical behavior of the measured current during the full anodization of a 75 nm Al film. The four different anodization phases are separated by dotted lines. The arrow indicates the time instant where the procedure should be stopped in order to prevent the full anodization of the aluminum film.

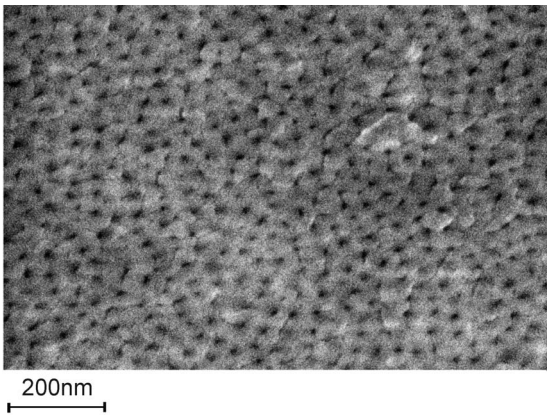

FIG. 6. Top view SEM micrograph of a partially anodized aluminum film.

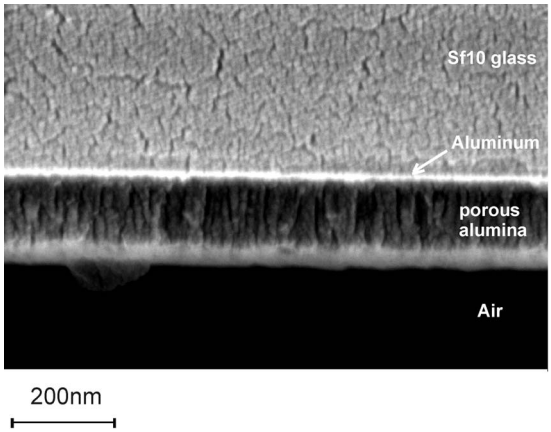

FIG. 7. Cross-sectional SEM micrograph of the porous alumina enhanced SPR sensor.

section SEM micrographs (Fig. 7) and as we will demonstrate later, it is also confirmed by fits to the SPR data.

Experimental SPR curves were acquired using the custom made SPR apparatus previously described.[22] An He–Ne laser ($\lambda = 632.8$ nm) was used as light source. The SF10 glass slides supporting the Al/p-Al_2O_3 layers are mounted on the face of a SF10 glass prism, using a refractive index matching fluid.

It is well established[23] that self-assembled monolayers (SAM) of about 2 nm thickness can be formed on alumina surfaces by liquid phase deposition of octadecyl-phosphonic acid (ODP). In order to study the effect of molecular adsorption on the p-Al_2O_3 pore walls, we prepared 0.1 wt % ethanol solutions of ODP (supplied by Alfa Aesar) and brought it into contact with the sensing surface with the aid of a suitable Teflon® cell. SAM formation was left to take place for 24 h at room temperature. For *ex situ* measurements, after the reaction, the surface was thoroughly rinsed with ethanol and then blown dry with nitrogen gas. Fittings of SPR curves before and after ODP SAM formation on planar alumina

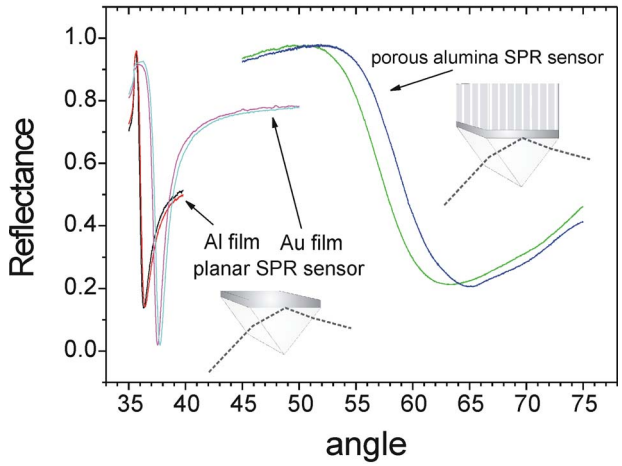

FIG. 8. (Color online) Experimental SPR curves (left) classic SPR, [aluminum (15 nm)/alumina (3.5 nm)] and (gold 48 nm), before and after ODP SAM and 18-alkanethiolate SAM formation respectively (right) p-Al_2O_3 enhanced SPR, aluminum (8.5 nm)/p-Al_2O_3 (118 nm), before and after ODP SAM formation. Note the large shift of the SPR curve that is induced by ODP adsorption on the pore walls.

surfaces (Fig. 8, left) suggest that the final layer has a thickness of 2.2 nm.

For comparison of the widely used planar Au film SPR sensor with the p-Al_2O_3 assisted SPR sensor, we have also conducted *ex situ* SAM formation experiments of 18-alkanethiolate molecules (supplied by Alfa Aesar) on 48 nm Au films from 0.01 wt % ethanol solutions. The replacement of ODP in this experiment was necessary as this molecule does not form a SAM on gold. The choice of 18-alkanethiolate is based on the fact that these molecules have the same number of carbon units as ODP while the thiol end group leads to the formation of a chemical bond with the gold surface. The Au SPR curve shift of 0.20° (Fig. 8, left) corresponds to a thiol SAM layer thickness of 2.1 nm, in excellent agreement with previous SPR studies.[24]

IV. RESULTS AND DISCUSSION

Since the ODP molecules are much smaller than the pore diameter, we assume that they are able to diffuse inside the pore structure. We have performed ODP SAM formation experiments for various p-Al_2O_3 layer thicknesses in the range of 110–155 nm. Representative *ex situ* SPR measurements of the Al/p-Al_2O_3 setup before and after ODP SAM formation on the pore walls are presented in Fig. 8 (right). In all cases, we observe a large curve shift that is induced by the SAM's presence. This shift is at least one order of magnitude larger than the one observed for the Al or Au planar geometry.

Curve fittings for the case of the bare p-Al_2O_3 layer (Fig. 8) give a p-Al_2O_3 thickness approximately 1.5 times larger than that of the preanodized Al film and a refractive index ($n_{p\text{-}Al_2O_3} \simeq 1.61$) which is lower than that of Al_2O_3 ($n_{Al_2O_3} \simeq 1.65$) in good agreement with c-MG theory Eq. (1) (using pore size and density values estimated by SEM). In all our experiments, there is a systematic deviation in the shift of the SPR curve from the theoretical prediction for a layer of 2.2 nm in the pore walls. This deviation is about $\simeq -10\%$, suggesting that the ODP shell thickness is slightly lower than 2.2 nm, equal to ~2.0 nm. This difference between adsorption on planar and porous alumina may be attributed to the curved nature of the pore's inner surface.

Overall, we have obtained very good fits to the experimental data (Fig. 9), while the use of the modified c-MG theory for the analysis of SPR data allowed for the determination of both, bare p-Al_2O_3 and ODP SAM layer characteristics. Based on these results, we argue that the proposed sensor and analysis scheme may be employed in a straightforward way for the detailed study of adsorption phenomena on the p-Al_2O_3 pore walls.

Nanoporous alumina adlayers may be easily integrated into existing commercially available SPR sensor technologies while cheaper sensors, based on this design may be manufactured. For biosensor applications, the pore walls may be decorated with appropriate molecules in order to resemble biointerfaces of interest.[11] Another advantage of this design is that the limited pore size may be used as a filter in a complex liquid environment, in order to probe selectively only some small target molecules of interest, having a size

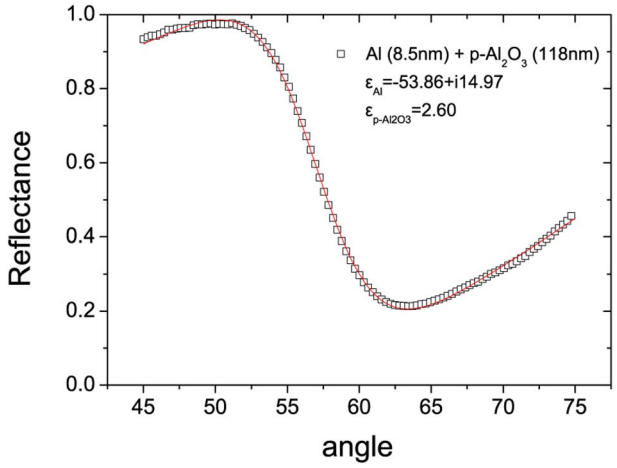

FIG. 9. (Color online) Experimental SPR curve of an aluminium/ p-Al_2O_3 system. The full line represents a fit to the experimental data. Values of film thicknesses and dielectric constants (inset) are obtained by the fitting procedure. Not all acquired experimental points are shown for reasons of clarity.

that permits their diffusion into the porous medium. Pore sizes may be easily tuned by the use of appropriate anodization conditions or by controlled postanodization chemical etching of the p-Al_2O_3 layer in phosphoric acid solutions in order to produce a sensor adapted to a specific molecular size.

It is well known that porous alumina is very sensitive to humidity.[25] Calculations based on Eq. (2) show that an adsorbed monolayer of water molecules on the inner pore surface, may induce SPR curve shifts, of the order of 0.1°–0.2°. This response suggests that the p-Al_2O_3 assisted SPR sensor may find use in humidity and/or gas detection applications. However the possibility for humidity or specific gas detection should be explored by performing measurements under appropriate and accurately controlled atmosphere.

The proposed setup is not limited to aluminum films for the plasmon excitation. Also gold films with a fully anodized p-Al_2O_3 overlayer can be used. However, this setup requires a proper ultrathin transparent adhesive layer between the glass substrate and the gold film in order to avoid delamination during the anodization procedure.[9] The use of a gold film should also provide better control of the thickness and uniformity of the plasmon supporting layer.

Finally, we would also like to mention that apart from its sensor applications, the proposed structure may also find use in the study of photonic band gap phenomena associated with the propagation of SP at the interface between a metal and a two-dimensional periodically patterned dielectric.[26] For highly ordered pore structures (that can be achieved by two-step anodization procedures) and certain interpore distances, SP reflection and transmission effects at refractive index steps may lead to a change of SP dispersion relation which reflects the prohibition of surface modes over a range of frequencies.

V. CONCLUSION

In summary, we have investigated the efficiency of a simple to fabricate nanoporous alumina assisted SPR sensor.

We described the conditions under which the technique may offer great signal enhancement comparing to "classic" SPR sensors. Fabrication steps are outlined while the *ex situ* experimental investigation of phosphonate SAM formation on the porous alumina walls confirmed that the proposed setup provides a highly sensitive response that may extend the implementation of the technique in applications demanding very high accuracy. Work underway includes in-situ adsorption studies, investigation of the sensor's applicability as a gas detector, and further theoretical and experimental studies to optimize performance.

ACKNOWLEDGMENT

The authors thank Dr. V. Dracopoulos for assistance with SEM and Professor Chris Toprakcioglu for helpful discussions and comments on the manuscript.

[1]W. L. Barnes, A. Dereux, and T. W. Ebbesen, Nature (London) **424**, 824 (2003).
[2]H. Kretschmann and H. Raether, Z. Naturforsch. A **23**, 2135 (1968).
[3]W. Knoll, MRS Bull. **16**, 29 (1991).
[4]J. Homola, S. S. Yee, and G. Gauglitz, Sens. Actuators B **54**, 3 (1999).
[5]R. J. Green, R. A. Frazier, K. M. Shakesheff, M. C. Davies, C. J. Roberts, and S. J. B. Tendler, Biomaterials **21**, 1823 (2000).
[6]H. Masuda and K. Fukuda, Science **268**, 1466 (1995).
[7]K. Nielsch, J. Choi, K. Schwirn, R. B. Wehrspohn, and U. Gosele, Nano Lett. **2**, 677 (2002).
[8]Z. L. Xiao, C. Y. Han, U. Welp, H. H. Wang, W. K. Kwok, G. A. Willing, J. M. Hiller, R. E. Cook, D. J. Miller, and G. W. Crabtree, Nano Lett. **2**, 1293 (2002).
[9]P. Evans, W. R. Hendren, R. Atkinson, G. A. Wurtz, W. Dickson, A. V. Zayats, and R. J. Pollard, Nanotechnology **17**, 5746 (2006).
[10]Y. F. Mei, G. G. Siu, G. S. Huang, and X. L. Wu, Appl. Surf. Sci. **230**, 393 (2004).
[11]V. Proux-Delrouyre, J. M. Laval, and C. Bourdillon, J. Am. Chem. Soc. **123**, 9176 (2001).
[12]O. K. Varghese, D. Gong, W. R. Dreschel, K. G. Ong, and C. A. Grimes, Sens. Actuators B **94**, 27 (2003).
[13]M. Kokonou, A. G. Nassiopoulou, and K. P. Giannakopoulos, Nanotechnology **16**, 103 (2005).
[14]K. H. A. Lau, L. S. Tan, K. Tamada, M. S. Sander, and W. Knoll, J. Phys. Chem. B **108**, 10812 (2004).
[15]M. Durr, B. Menges, W. Knoll, A. Yasuda, and G. Nelles, Appl. Phys. Lett. **91**, 021113 (2007).
[16]Z.-M. Qi, I. Honma, and H. Zhou, Appl. Phys. Lett. **90**, 011102 (2007).
[17]D. H. Kim, K. H. A. Lau, J. W. F. Robertson, O.-J. Lee, U. Jeong, J. I. Lee, C. J. Hawker, T. P. Russell, J. K. Kim, and W. Knoll, Adv. Mater. (Weinheim, Ger.) **17**, 2442 (2005).
[18]W. L. Barnes, J. Opt. A, Pure Appl. Opt. **8**, S87 (2006).
[19]J. E. Spanier and I. P. Herman, Phys. Rev. B **61**, 10437 (2000).
[20]P. G. Miney, P. E. Colavita, M. V. Schiza, R. J. Priore, F. G. Haibach, and M. L. Myrick, Electrochem. Solid-State Lett. **6**, B42 (2003).
[21]During our experiments we have encountered some minor issues concerning Al and *P*-Al film lateral inhomogeneity over macroscopic distances (several millimeters) that may distort the acquired SPR curves. The potential use of a hemicylindrical prism that samples a constant small portion of the film surface should eliminate this effect.
[22]A. G. Koutsioubas, N. Spiliopoulos, D. Anastassopoulos, A. A. Vradis, C. Toprakcioglu, and G. D. Priftis, J. Polym. Sci., Part B: Polym. Phys. **44**, 1580 (2006).
[23]E. Hoque, J. A. DeRose, P. Hoffmann, H. J. Mathieu, B. Bhushan, and M. Cichomski, J. Chem. Phys. **124**, 174710 (2006).
[24]K. A. Peterlinz and R. Georgiadis, Langmuir **12**, 4731 (1996).
[25]M. Sato, T. Yamamoto, T. Meguro, and K. Tamanouchi, Sens. Actuators B **20**, 205 (1994).
[26]J. Yoon, G. Lee, S. H. Song, C.-H. Oh, and P.-S. Kim, J. Appl. Phys. **94**, 123 (2003).
[27]Such porosity values have been reported for different anodization conditions of thin aluminium films (Ref. 13). Large pore size can be obtained by postanodization etching.